The Plant Cell, Vol. 25: 1383–1399, April 2013, www.plantcell.org

Autophagy Contributes to Leaf Starch Degradation[C][W]

Yan Wang,[a,1] Bingjie Yu,[a,1] Jinping Zhao,[a] Jiangbo Guo,[a,2] Ying Li,[b] Shaojie Han,[a] Lei Huang,[b] Yumei Du,[a] Yiguo Hong,[c] Dingzhong Tang,[d] and Yule Liu[a,3]

[a] MOE Key Laboratory of Bioinformatics, School of Life Sciences, Tsinghua University, Beijing 100084, China
[b] Center of Biomedical Analysis, Tsinghua University, Beijing 100084, China
[c] Research Centre for Plant RNA Signaling, School of Life and Environmental Sciences, Hangzhou Normal University, Hangzhou 310036, China
[d] State Key Laboratory of Plant Cell and Chromosome Engineering, Institute of Genetics and Developmental Biology, Chinese Academy of Sciences, Beijing 100101, China

Transitory starch, a major photosynthetic product in the leaves of land plants, accumulates in chloroplasts during the day and is hydrolyzed to maltose and Glc at night to support respiration and metabolism. Previous studies in *Arabidopsis thaliana* indicated that the degradation of transitory starch only occurs in the chloroplasts. Here, we report that autophagy, a nonplastidial process, participates in leaf starch degradation. Excessive starch accumulation was observed in *Nicotiana benthamiana* seedlings treated with an autophagy inhibitor and in autophagy-related (*ATG*) gene-silenced *N. benthamiana* and in *Arabidopsis atg* mutants. Autophagic activity in the leaves responded to the dynamic starch contents during the night. Microscopy showed that a type of small starch granule-like structure (SSGL) was localized outside the chloroplast and was sequestered by autophagic bodies. Moreover, an increased number of SSGLs was observed during starch depletion, and disruption of autophagy reduced the number of vacuole-localized SSGLs. These data suggest that autophagy contributes to transitory starch degradation by sequestering SSGLs to the vacuole for their subsequent breakdown.

INTRODUCTION

In plants, most storage carbohydrates exist in the form of starch. According to temporal and spatial differences in its biosynthesis, starch can be classified into two types: transitory starch, which occurs in photosynthetic organs and is also called leaf starch, and reserve starch, which occurs in storage organs. Whereas reserve starch can be stored for months or even years, transitory starch accumulates in chloroplasts of leaf cells during the day and is depleted during the subsequent night. The neutral sugars produced by the degradation of leaf starch, mainly maltose and Glc, are then exported from the chloroplast to the cytosol to ensure optimal carbon supply for continued nocturnal plant growth. In addition to providing substrates for cellular respiration, a portion of the sugars is converted into transportable metabolites, mainly in the form of Suc, and transported to sink organs, such as roots, tubers, or seeds, for further starch biosynthesis (Fettke et al., 2009; Santelia and Zeeman, 2011).

Studies in *Arabidopsis thaliana* suggest that leaf starch degradation occurs in chloroplasts. Reversible starch phosphorylation and glucan hydrolysis are two necessary steps in the degradation process (Zeeman et al., 2010). Two types of glucan water dikinase are responsible for starch phosphorylation. GWD (for glucan water dikinase) phosphorylates the C6 position of glucosyl residues, and PWD (for phosphoglucan water dikinase) phosphorylates the C3 position of prephosphorylated glucan chains (Ritte et al., 2006). Mutation in either of these dikinase genes results in a starch-excess phenotype, indicating that glucan phosphorylation is essential for the normal metabolism of leaf starch (Yu et al., 2001; Baunsgaard et al., 2005; Kötting et al., 2005). Moreover, the leaves of *Arabidopsis* mutants lacking the phosphoglucan phosphatase STARCH EXCESS4 or its close homolog LIKE SEX FOUR1 retain high starch levels at dawn (Kötting et al., 2009; Comparot-Moss et al., 2010). Whereas starch phosphorylation disrupts the semicrystalline lamellae at the granule surface, starch dephosphorylation eliminates phosphate groups, which prevents exoamylase from acting on the glucan chain (Yu et al., 2001; Kötting et al., 2009; Zeeman et al., 2010). In *Arabidopsis*, the β-amylases BAM1 and BAM3 and debranching enzymes ISOAMYLASE3 and LIMIT DEXTRINASE are active hydrolyzing enzymes that act on leaf starch (Kaplan and Guy, 2005; Wattebled et al., 2005; Delatte et al., 2006; Fulton et al., 2008). β-Amylases catalyze the hydrolysis of α-1,4-glycosidic linkages and release maltose from the exposed nonreducing ends of glucan chains, whereas debranching enzymes hydrolyze α-1,6-glycosidic bonds and remove branches mainly from amylopectin (Zeeman et al., 2010).

Autophagy is a bulk degradation process by which eukaryotic cells recycle intracellular components, such as protein aggregates

[1] These authors contributed equally to this work.
[2] Current address: School of Mathematics, Physics, and Biological Engineering, Inner Mongolia University of Science and Technology, Baotou 014010, China.
[3] Address correspondence to yuleliu@mail.tsinghua.edu.cn.
The author responsible for distribution of materials integral to the findings presented in this article in accordance with the policy described in the Instructions for Authors (www.plantcell.org) is: Yule Liu (yuleliu@mail.tsinghua.edu.cn).
[C] Some figures in this article are displayed in color online but in black and white in the print edition.
[W] Online version contains Web-only data.
www.plantcell.org/cgi/doi/10.1105/tpc.112.108993

and organelles (Klionsky and Emr, 2000). Three types of autophagy have been defined: macroautophagy, microautophagy, and chaperone-mediated autophagy (Massey et al., 2004). Macroautophagy (referred to hereafter as autophagy), the major type of autophagy, occurs when cytoplasmic constituents are engulfed by double-membrane vesicles termed autophagosomes and delivered to the lysosomes or vacuoles for breakdown and turnover. Autophagy is evolutionarily conserved from yeast to mammals. Most of the autophagy-related (*ATG*) genes identified in yeast have homologs in mammals and plants (Hanaoka et al., 2002; Levine and Klionsky, 2004; Han et al., 2011). Autophagy is known to function as an adaptation to starvation in mammals and yeast and also assists plants in surviving nutrient limitation stress (Aubert et al., 1996; Moriyasu and Ohsumi, 1996). In addition, autophagy is reported to be involved in plant development, functioning in processes such as root tip cell growth and differentiation (Inoue et al., 2006; Yano et al., 2007), floret development in wheat (*Triticum aestivum*; Ghiglione et al., 2008), tracheary element differentiation (Kwon et al., 2010), and chloroplast degradation in senescent leaves (Ishida et al., 2008; Wada et al., 2009; Izumi et al., 2010). Previous research conducted by our group and others demonstrated that autophagy also participates in plant innate immunity (Liu et al., 2005; Patel and Dinesh-Kumar, 2008; Yoshimoto et al., 2009; Hofius et al., 2011; Lai et al., 2011; Lenz et al., 2011; Wang et al., 2011) and responses to a variety of abiotic stresses, including high salinity, drought, and oxidative stress (Xiong et al., 2007; Liu et al., 2009). Previous ultrastructural observations of cotyledons of germinated *Vigna mungo* seeds suggest that microautophagic machinery may be involved in the degradation of reserve starch (Toyooka et al., 2001). Blocking the metabolism of starch breakdown products in both *maltose excess1* (*mex1*) and the *disproportionating enzyme1* (*dpe1*) *mex1* double mutant triggers chloroplast degradation, suggesting a possible link between carbohydrate metabolism and autophagy (Stettler et al., 2009; Cho et al., 2010). However, it was hitherto unknown whether autophagy plays a role in transitory starch degradation. In this study, we report that autophagy does indeed contribute to leaf starch degradation and reveal a role of basal autophagy in plants.

RESULTS

3-Methyladenine Treatment Results in Starch-Excess Phenotype

The class III phosphatidylinositol 3-kinase (PI3K) together with ATG6 and other regulatory proteins forms a protein complex that is essential for the nucleation of autophagosomes (Xie and Klionsky, 2007; Mizushima et al., 2011). The well-characterized autophagy inhibitor 3-methyladenine (3-MA) specifically inhibits PI3K activity and has been widely used to decipher the roles of autophagy in mammalian and plant cells (Seglen and Gordon, 1982; Blommaart et al., 1997; Takatsuka et al., 2004; Inoue et al., 2006). To investigate whether autophagy participates in leaf starch degradation, we treated *Nicotiana benthamiana* seedlings with 3-MA (5 mM). The seedlings germinated on rich Murashige and Skoog (MS) medium containing 3-MA showed reduced growth compared with the control seedlings (see Supplemental Figure 1 online). We determined the leaf starch content of these seedlings using iodine staining (Figure 1A). As expected, the control seedlings synthesized leaf starch during the day and mobilized it at night. By contrast, the leaves of seedlings grown on plates containing 3-MA showed increased starch levels at the end of both the day and night. Quantification of starch in whole seedlings showed similar results (Figure 1B). Thus, autophagy may be involved in starch depletion in *N. benthamiana* leaves.

Autophagy-Related Genes and Autophagic Activity in the Leaf Were Induced During the Night

To further investigate the involvement of autophagy in starch degradation at night, we examined the expression of *ATG* genes in *N. benthamiana* at different time points during the night. The transcript abundance of six *ATG* genes, including *ATG2*, *ATG4*, *ATG6*, *ATG7*, *ATG9*, and *PI3K*, was analyzed by real-time RT-PCR. The expression levels of all these *ATG* genes, other than *ATG2* and *ATG4*, were rapidly altered during the first 4 h of adaptation to darkness (Figure 2). *ATG6* and *ATG9* expression increased, peaked at 2 h after darkness, and then declined to basal levels by the end of the night. *PI3K* and *ATG7* also showed enhanced expression during the night, but expression peaked

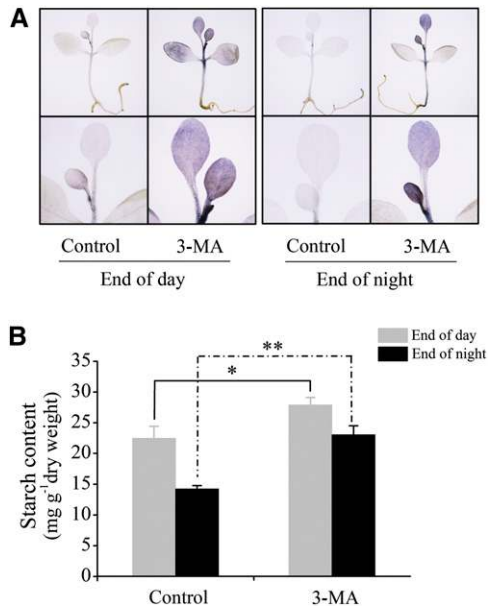

Figure 1. 3-MA Treatment Results in a Starch-Excess Phenotype.

(A) Iodine staining of 3-MA–treated seedlings. Two-week-old *N. benthamiana* seedlings germinated on MS plates containing or not containing 5 mM 3-MA were harvested at the end of the day and night for determination of starch content.

(B) Quantification of starch in 3-MA–treated seedlings. Approximately 30 seedlings were harvested and regarded as one sample for the starch quantification test. Values are means ± SE of four replicate samples. Student's *t* test was applied to determine statistically significant differences (*P <0.05; **P <0.01).

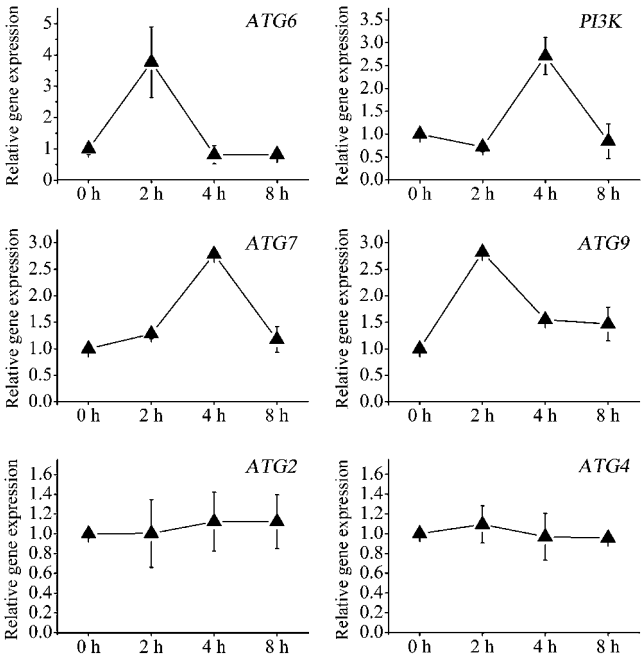

Figure 2. Transcript Pattern of Autophagy-Related Genes during the Night.

Real-time RT-PCR analysis was performed using total RNA isolated from leaves at the indicated time points. Expression data relative to 0 h were normalized to that of actin. Values are means ± SE from two independent experiments.

after 4 h in darkness. Thus, the transcript levels of these *ATG* genes displayed diverse dynamic alterations during the night, suggesting that the cellular machinery underlying autophagy was active.

To test this idea, we adopted three classic approaches to monitoring autophagosome formation in leaves during the night. We first used monodansylcadaverine (MDC), an acidotropic dye widely used in mammals and plants for detecting autophagic structures (Biederbick et al., 1995; Munafó and Colombo, 2001; Contento et al., 2005), as a probe to identify autophagosomes. *ATG6*-silenced plants (see Supplemental Figure 2 online) served as the negative control. MDC-positive autophagic structures were observed in the mesophyll cells of wild-type *N. benthamiana* plants (Figures 3A and 3B) but rarely in those of the *ATG6*-silenced plants (see Supplemental Figure 3A online). Generally, the MDC-stained autophagosomes moved randomly in the central vacuole in the form of individual or aggregated autophagic structures (Figure 3B). MDC-stained autophagosomes that exhibit little motion were also observed around the chloroplast envelope and were probably located in the cytoplasm (Figure 3B). Quantitative analysis of the MDC-stained autophagic structures in leaves showed that autophagosome formation largely increased within the first 4 h of exposure to darkness (~3.18-fold greater than at the beginning of the night) and returned to basal levels by the end of the night (Figure 3C).

To confirm these results, we used cyan fluorescent protein (CFP)–tagged tobacco (*Nicotiana tabacum*) ATG8f (CFP-ATG8f) as an autophagosome marker to monitor autophagy. The spherical and punctate structures labeled by fluorescent protein–tagged ATG8 are interpreted as being autophagosomes and their intermediates (Yoshimoto et al., 2004; Contento et al., 2005). Generally, the fluorescence resulting from CFP-ATG8f displayed cytosolic localizations in mesophyll cells (Figure 3D). The spherical or punctate structures labeled by CFP-ATG8f were observed in leaves subjected to 4 h of darkness, but fewer structures were observed in leaves exposed to 0 or 8 h of darkness (Figures 3D and 3E). These CFP-ATG8f–labeled structures were rarely seen in the *ATG6*-silenced plants (see Supplemental Figure 3B online). Furthermore, we used transmission electron microscopy (TEM) to monitor autophagic activity during the night. We observed both classic double-membrane autophagosomes in the cytoplasm and autophagic bodies with a single membrane in the vacuole (Figures 4A and 4B). In agreement with the results of MDC staining, both the CFP-ATG8f and TEM methods showed that the autophagic activity in leaves increased 3.51- and 3.39-fold, respectively, after 4 h of darkness and returned to basal levels at the end of the night (Figures 3F and 4C). Taken together, these data suggest that autophagic activity in the leaf is induced during the night.

Finally, we examined the dynamic changes in leaf starch content during darkness. Iodine staining and ultrastructural observations indicated that most of the leaf starch was depleted within the first 4 h of exposure to darkness (Figures 5A and 5B). This result was confirmed by quantification of starch content at different time points during the night (Figure 5C). About 70% of starch mobilized during the night was degraded within the first 4 h of darkness, whereas ~30% of starch was degraded in the last 4 h (Figure 5C). Moreover, both the size and average number of visible starch granules per chloroplast gradually diminished during the night (Figure 5B; see Supplemental Figure 4A online). As the number of starch granules per chloroplast is relatively constant throughout the night (Crumpton-Taylor et al., 2012), the reduced number of visible starch granules observed by TEM was possibly due to the diminished chances of observing small, shrinking starch granules in ultrathin sections. The temporal coincidence between starch degradation and autophagy upregulation implies that autophagy plays a role in leaf starch degradation during the night.

Silencing of *ATG* Genes Reduces Leaf Starch Degradation

ATG6 is an essential protein in the nucleation of autophagic vesicles, and silencing of *ATG6* eliminates autophagic activity in plants (Liu et al., 2005; Patel and Dinesh-Kumar, 2008). Using the iodine staining, we examined the accumulation of leaf starch in *ATG6*-silenced *N. benthamiana* grown under a 16-h-light/8-h-dark diurnal cycle. After 8 h of exposure to darkness, leaf starch reserves were almost exhausted in control plants, while excess starch was detected in *ATG6*-silenced plants (Figure 6A). Indeed, quantification of starch reserves in leaves at the end of the dark period confirmed the starch-excess phenotype in *ATG6*-silenced plant (Figure 6B). Moreover, TEM analysis showed that starch granules remained visible in the chloroplasts of *ATG6*-deficient leaves but not in those of nonsilenced control plants at

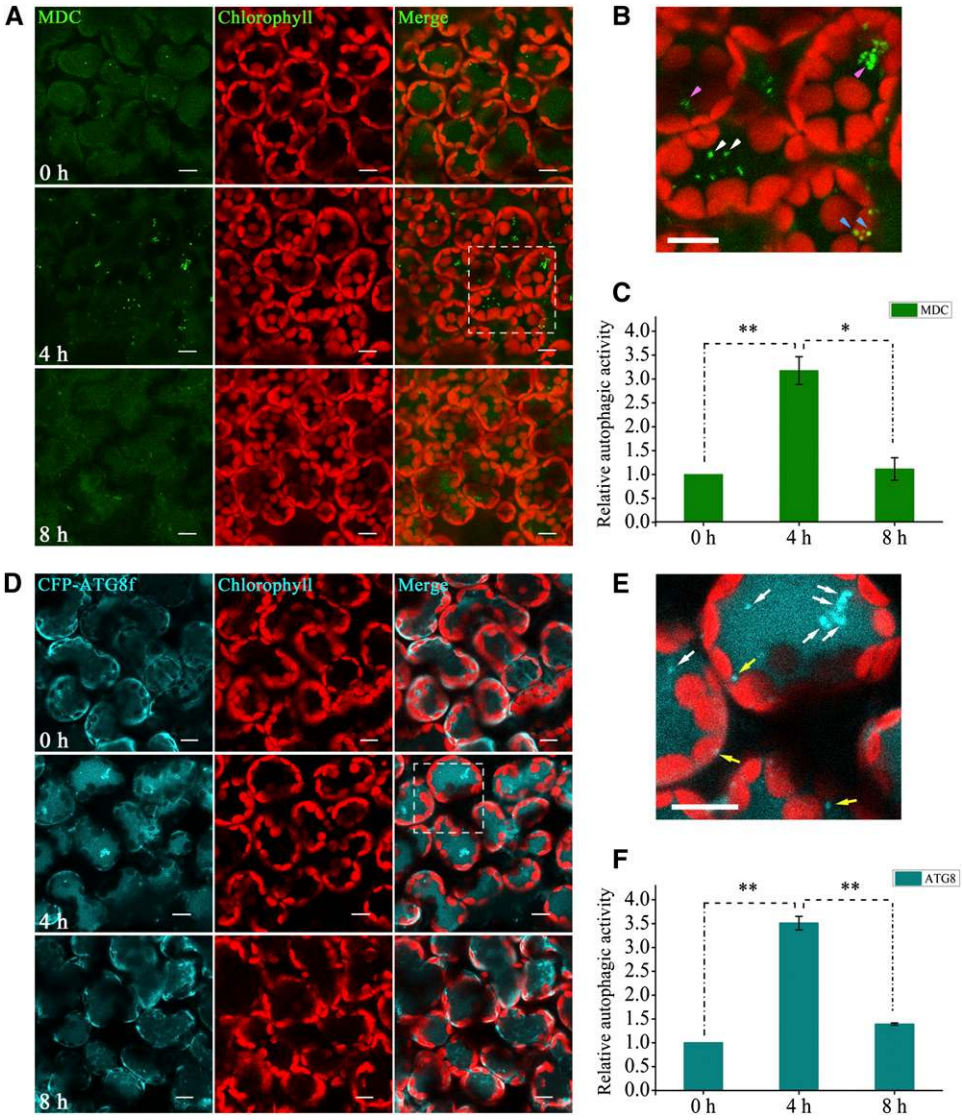

Figure 3. Visualization of Autophagy in Leaves in Night Conditions by Confocal Microscopy.

(A) to **(C)** Dynamic autophagic activity as revealed by MDC staining.

(A) MDC-stained autophagosomes in the leaves after various periods in darkness. MDC-labeled structures are in green and the chloroplasts are in red. Bars = 10 μm.

(B) Magnification of the mesophyll cells surrounded by a dashed line in **(A)**. MDC-stained autophagosomes are indicated by arrowheads. The white and magenta arrowheads indicate the individual and aggregated autophagic structures in the vacuole, respectively. The blue arrowheads refer to the autophagosomes in the cytoplasm. Bars = 10 μm.

(C) Relative autophagic activity normalized to the activity at the beginning of night. Quantification of the MDC-stained autophagosomes in leaves at each time point was performed to calculate the autophagic activity relative to that at time 0 h, which was set to 1. Over 300 mesophyll cells for each time point were used for the quantification. Values represent means ± SE from two independent experiments. Student's *t* test was applied to determine significant differences (*P < 0.05; **P < 0.01).

(D) to **(F)** Dynamic autophagic activity showed by autophagy marker CFP-ATG8f.

(D) Autophagosomes labeled by CFP-ATG8f in leaves at different time points after dark treatment. CFP-ATG8f fusion proteins are in cyan, and chloroplasts are in red. Bars = 10 μm.

(E) Magnification of the mesophyll cells surrounded by a dashed line in **(D)**. Autophagosomes labeled by CFP-ATG8f are indicated by arrows. Yellow arrows indicate autophagosomes in the cytoplasm. White arrows indicate autophagosomes in the vacuole. Bars = 10 μm.

(F) Relative autophagic activity normalized to the activity at the beginning of night. Quantification of the CFP-ATG8–labeled autophagosomes in leaves at each time point was performed to calculate the autophagic activity relative to that at time 0 h, which was set to 1. More than 100 mesophyll cells for each time point were used for the quantification. Values represent means ± SE from two independent experiments. Student's *t* test was used to determine significant differences (**P < 0.01).

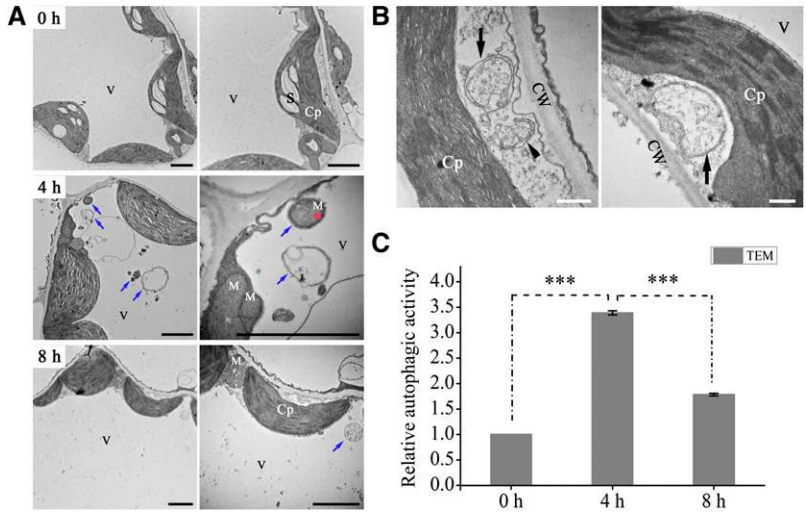

Figure 4. TEM of Dynamic Autophagic Activity in Leaves during the Night.

(A) Representative TEM images of autophagic structures at different time points after dark treatment. Lots of autophagic bodies (blue arrows) appeared in the central vacuole of mesophyll cells after 4 h of exposure to darkness, but fewer were visible at other time points. The red asterisk indicates a mitochondrion that has entered the vacuole. Cp, chloroplast; M, mitochondrion; S, starch; V, vacuole. Bars = 2.5 μm.

(B) Representative ultrastructure of autophagosomes observed in the cytoplasm of mesophyll cells. In addition to the classic double-membrane autophagosomes (black arrows), an isolation membrane (autophagosome precursor, indicated by black arrowhead) was observed. CW, cell wall. Bars = 500 nm.

(C) Relative autophagic activity normalized to the activity at the beginning of the night. Approximately 20 cells were used to quantify autophagic structures. Values represent means ± SE from two independent experiments. Student's *t* test was applied to indicate significant differences (***P < 0.001).

the end of the dark period (Figure 6C). In addition, we analyzed the leaf starch content at the end of the 16-h illumination period by iodine staining and found that a higher level of starch accumulated in *ATG6*-deficient plants than in nonsilenced controls (see Supplemental Figure 5A online).

To exclude the possibility that the higher level of starch accumulation in *ATG6*-silenced plants after dark treatment was caused by enhanced starch synthesis, we performed a destarch assay as described previously (Critchley et al., 2001). Plants were subjected to 60 h of complete darkness, at which point starch reserves had been almost completely remobilized from the leaves, and then transferred to a normal 16-h-light/8-h-dark cycle. The starch content of leaves during the next two regular cycles was quantitatively determined (see Supplemental Figure 5B online). As expected, almost no starch was detectible in *ATG6*-silenced and nonsilenced plants after 60 h of darkness, and no noticeable difference occurred in the amount of starch synthesized by leaves in the next 2 d. However, only 55.3 and 40.6% of starch synthesized during the day was consumed in the next two nights in *ATG6*-silenced plants, in contrast with the 87.1 and 81.6% of starch consumed in nonsilenced plants (see Supplemental Figure 5C online). These results illustrate that a reduction in starch degradation led to the starch-excess phenotype of *ATG6*-deficient plants. Indeed, the imbalance in starch synthesis and degradation in *ATG6*-silenced plants was consistent with the classic phenotype of starch-excess mutants that had defective starch degradation (Zeeman et al., 1998a; Critchley et al., 2001; Chia et al., 2004; Niittylä et al., 2004, 2006; Fulton et al., 2008; Comparot-Moss et al., 2010).

To further test the involvement of autophagy in leaf starch degradation, we silenced other *ATG* genes, including *ATG2*, *ATG3*, *ATG5*, *ATG7*, *PI3K*, and *VTI12*. RT-PCR analysis confirmed the reduced expression of each gene (see Supplemental Figure 2 online). Autophagosome formation was also reduced in these silenced plants (see Supplemental Figure 6 online). More importantly, silencing of these genes resulted in reduced starch degradation, as observed in *ATG6*-silenced plants, although various degrees of starch accumulation were observed (Figures 7A and 7B). These results suggest that autophagy contributes to leaf starch degradation during the night.

Small Starch Granule-Like Structures Are Observed Outside the Chloroplast

Previous studies indicated that leaf starch degradation occurs in the chloroplast (Zeeman et al., 2010). However, our results suggest that autophagy, a process that occurs in the cytoplasm, is involved in leaf starch degradation. Thus, it is unclear how autophagy contributes to chloroplast-localized leaf starch degradation. To investigate this, we constructed yellow fluorescent protein (YFP)–tagged granule-bound starch synthase I (GBSSI-YFP), a starch granule marker, to monitor changes of starch granules during the night. GBSSI is responsible for amylose synthesis, and a GBSSI-YFP fusion protein was previously used as a marker of starch granules in plants (Szydlowski et al., 2009; Bahaji et al., 2011). GBSSI-YFP transiently expressed in *N. benthamiana* mesophyll cells localized mainly in starch granules (restricted fluorescence on spherical or oval-shaped structures)

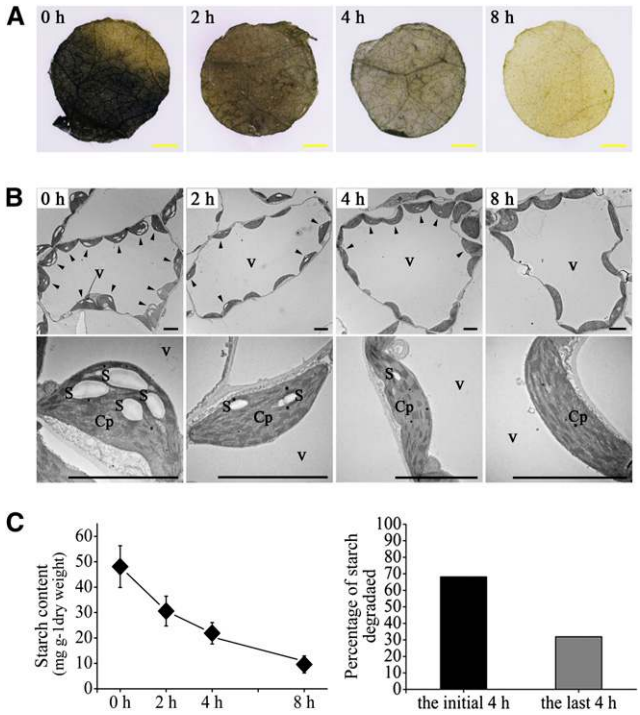

Figure 5. Starch Content Declined during the Night.

(A) Leaf discs stained with iodine solution reveal the decreased starch content during the night. Four time points (0, 2, 4, and 8 h after dark treatment) were selected for monitoring the starch content. Bars = 1 mm.
(B) Ultrastructural analysis of mesophyll cells indicates changes of starch granules during the night. The percentage of chloroplasts with visible starch granules (black arrowheads) in a mesophyll cell declined (top panel). The size and number of visible starch granules per chloroplast also diminished (bottom panel). Cp, chloroplast; S, starch; V, vacuole. Bars = 5 μm.
(C) Quantification of leaf starch contents during the night (left panel) and determination of the percentage of starch degraded in different time periods (right panel). Three replicate leaf samples for each time point were used in the starch quantification. Values are means ± SE. The percentage of starch degraded in the initial and last 4 h was determined according to the starch content measured at each time point (left panel).
[See online article for color version of this figure.]

rather than in the chloroplast stroma (diffuse fluorescence in the total chloroplast volume) during the day (Figure 8A, 0 h; Figures 8B and 8C). Along with the dark treatment, both the density of restricted fluorescence and the number of chloroplasts exhibiting restricted fluorescence significantly decreased (Figure 8A). Almost no YFP fluorescence was detected in leaves at the end of the dark period (Figure 8A, 8 h), consistent with the previous report that GBSSI released from degraded starch granules would eventually be destroyed (Smith et al., 2004). However, it seemed that the destruction of GBSSI-YFP fusion proteins was not instantaneous because not only restricted fluorescence on granules but also weak diffuse YFP fluorescence in the stroma was observed in leaf samples exposed to darkness for 2 and 4 h (Figure 8A). The diminished restricted fluorescence of GBSSI-YFP finely mimicked the changes in starch content during the dark period (Figure 5), which further suggested the feasibility of using GBSSI-YFP as a starch granule marker. As leaf starch degradation had been thought to occur only in the chloroplast, starch granules would not be expected to appear outside of normal chloroplasts. However, some fluorescently labeled particle-like structures with an average diameter of 0.47 μm were observed around the chloroplast envelope when the leaves were placed in darkness for 2 or 4 h (Figure 8D). These particle-like

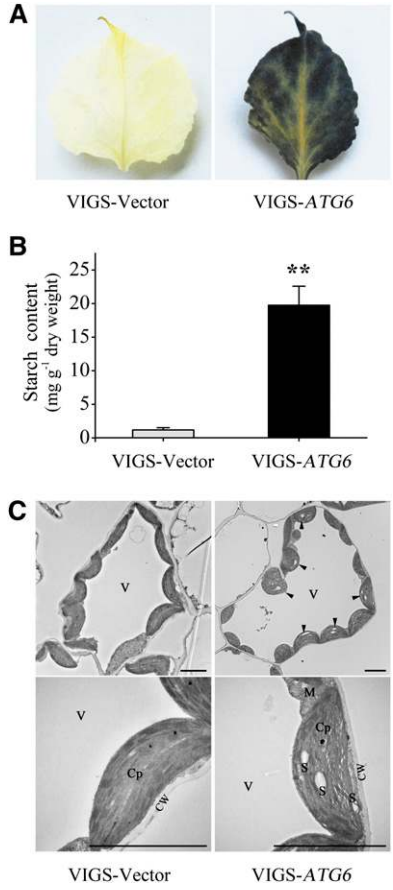

Figure 6. Starch-Excess Phenotype in *ATG6*-Silenced *Nicotiana benthamiana*.

(A) Iodine staining of leaves from *ATG6*-silenced and nonsilenced plants. Leaves were harvested at the end of the night for detection of starch content. Starch was almost exhausted in control leaves but was readily detected in the *ATG6*-silenced leaves. These results were reproduced in 10 independent experiments using two to three leaves in each experiment. Representative results are presented.
(B) Quantification of leaf starch content in *ATG6*-silenced and nonsilenced plants. Values are means ± SE from three replicate leaf samples. Two asterisks indicate a significant difference ($P < 0.01$; Student's *t* test).
(C) Ultrastructural analysis of starch accumulation in mesophyll cells. At the end of the night, almost no starch granules were visible in the chloroplasts of control leaves, whereas starch granules were still present in the chloroplasts (arrowheads) of *ATG6*-silenced leaves. Cp, chloroplast; CW, cell wall; M, mitochondrion; S, starch; V, vacuole. Bars = 5 μm.
[See online article for color version of this figure.]

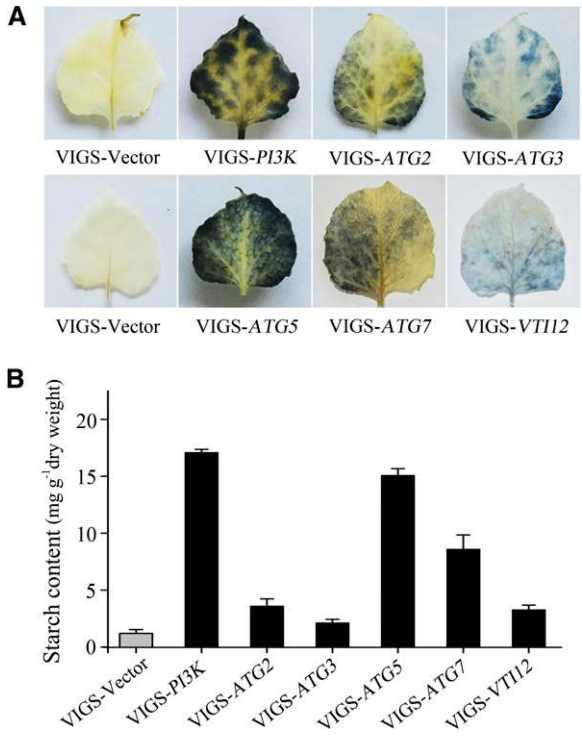

Figure 7. Silencing of Other *ATG* Genes Leads to Starch Accumulation at the End of the Night.

(A) Iodine staining of leaves from other *ATG* gene-silenced and non-silenced plants. Results were reproduced in more than three independent experiments using two to three leaves per experiment. Representative results are presented.

(B) Quantification of leaf starch in other *ATG* gene-silenced and non-silenced plants. Values are means ± SE from at least two replicate samples.

[See online article for color version of this figure.]

structures usually exhibited more restricted and intense fluorescence than the GBSSI-YFP in chloroplast stroma. Occasionally, such structures were seen in the vacuole (Figure 8E, 4 h; Figure 8F). This result suggests that starch components may occur outside the chloroplast.

In our electron microscopy analysis of *N. benthamiana* leaves, we found some small starch granule-like structures (SSGLs) in the cytoplasm and central vacuole of mesophyll cells after 2 and 4 h of exposure to darkness (Figure 9). This kind of structure was rarely observed in leaves harvested at the end of the day or night. The SSGLs had similar electron densities and appearances as those of normal transitory starch granules localized in the chloroplast but were much smaller. Whereas the normal transitory starch granules formed at the end of the light period were ~1 to 2 μm in diameter (see Supplemental Figure 4B online), similar to those in *Arabidopsis* (Crumpton-Taylor et al., 2012), most SSGLs had a diameter of <0.5 μm (see Supplemental Figure 4C online), similar to the particle-like structures labeled by GBSSI-YFP (Figure 8). A layer of membranous coating was usually observed at the periphery of the SSGLs (Figures 9B to 9D). In the vacuole, three types of SSGLs were observed, including (1) SSGLs engulfed by a single- or double-membrane vesicle (Figure 9B), (2) SSGLs located directly in the vacuole (Figure 9C), and (3) SSGLs that had almost completely degraded (Figure 9D).

To confirm that the SSGLs observed under TEM were indeed starch components, we stained the sections using the periodic acid–thiocarbohydrazide–silver proteinate (PA-TCH-SP) staining method (Thiery, 1967), which has been widely used in histochemical localization of neutral polysaccharides in mammals, bacteria, fungi (Braña et al., 1980; Lo et al., 1987; Yoshikawa et al., 1988), and starch granules in plant leaves (Zeeman et al., 1998b). As expected, no silver grains were observed in the control sections stained with TCH-SP or PA-SP or SP (see Supplemental Figure 7 online). However, in the sections stained with PA-TCH-SP, numerous silver grains were present on the surfaces of normal chloroplast-localized starch granules (Figures 10A and 10C). Moreover, SSGLs in the cytoplasm and vacuole were silver stained, and all three types of SSGLs were observed in the vacuole (Figure 10B; see Supplemental Figure 7 online). Some diffuse silver depositions with less intensity were often observed around the SSGLs (Figure 10B; see Supplemental Figure 7 online). We supposed that these depositions were the stained glucans released from the SSGLs due to the disruption of the semicrystalline lamellae and hydrolysis of starch by the degrading enzymes.

Taken together, these data suggest that the SSGLs outside the chloroplast are indeed starch components.

SSGL Structures Could Be Delivered to the Vacuole through Autophagy

To investigate whether autophagy contributes to the delivery of SSGLs to the vacuole, we performed a colocalization assay of SSGLs and autophagosomes. SSGLs labeled with GBSSI-YFP and autophagosomes labeled with CFP-ATG8f colocalized in the cytoplasm and central vacuole (Figure 8E, 4 h; Figure 8F). Furthermore, we captured the dynamic process of autophagosomes appearing at the chloroplast envelope and delivering SSGLs into the vacuole (Figure 8F). Ultrastructural observations revealed SSGLs engulfed by a single- or double-membrane vesicle in the vacuole, which resembled autophagic bodies (Figures 9 and 10; see Supplemental Figure 7 online). Thus, the three types of SSGLs might represent different degradation statuses of SSGLs upon transport into the vacuole through the autophagic pathway (Figures 9 and 10; see Supplemental Figure 7 online). In particular, the first type of SSGLs represents the typical status of small starch granules sequestered in autophagic bodies. Furthermore, we used TEM to determine the number of SSGLs present in the vacuole. Silencing of *ATG6* markedly reduced the number of vacuole-localized SSGLs in leaves exposed to darkness (Figure 10D). These data suggest that autophagy delivers SSGLs into vacuoles for subsequent degradation.

Stromules May Function as Exit Channels for SSGL Structures

The occurrence of SSGLs at the chloroplast envelope and in the vacuole raises an interesting question about how these

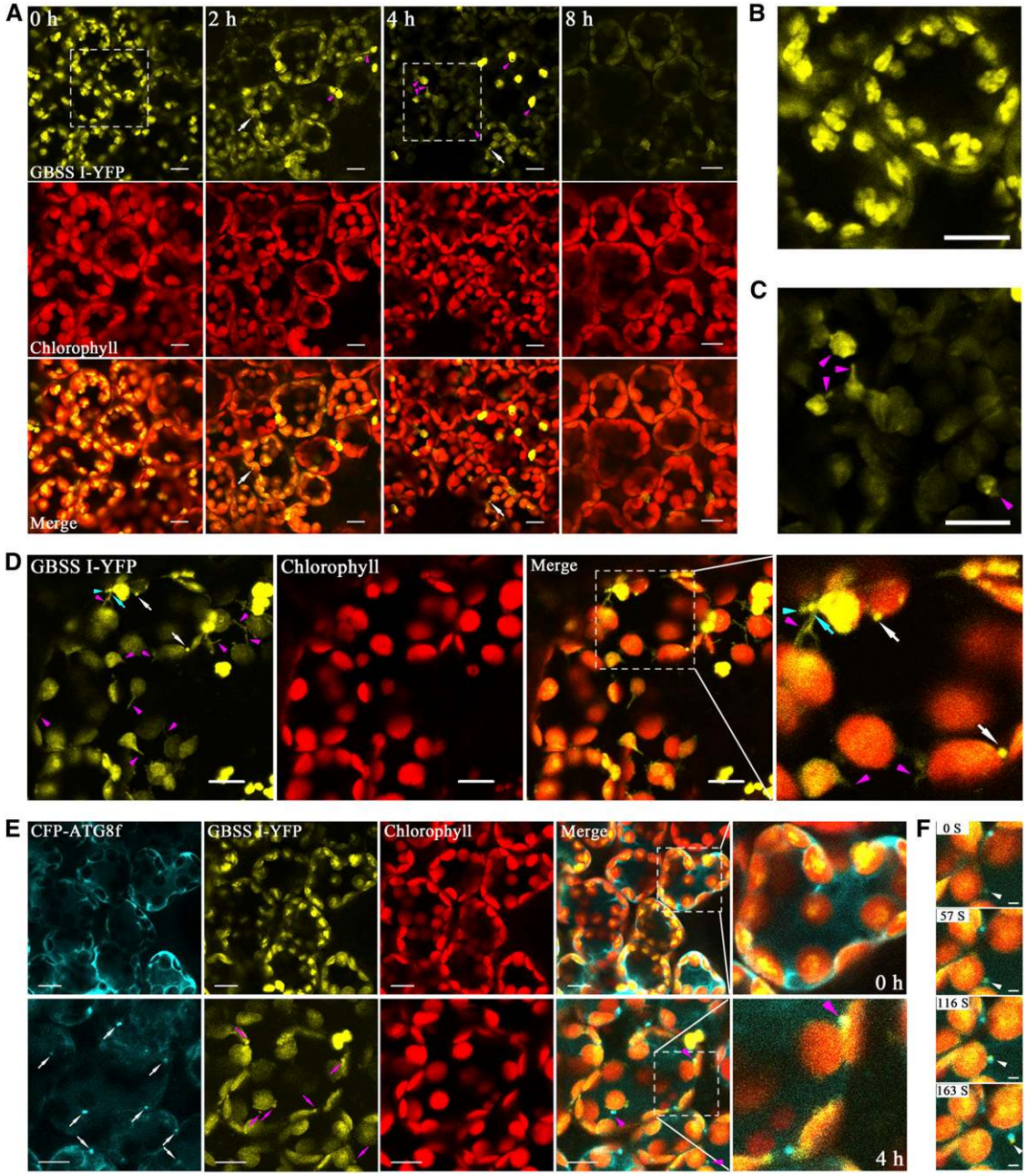

Figure 8. Confocal Microscopy of SSGLs Labeled by the Starch Granule Marker GBSSI-YFP.

(A) to **(C)** GBSSI-YFP could be used as a starch granule marker. Bars = 10 μm.

(A) GBSSI-YFP transiently expressed in leaves of *N. benthamiana* plants at different time points during the night. At the beginning of the night (0 h), GBSSI-YFP localized mainly on the starch granules in the chloroplasts. As the night progressed, the restricted fluorescence of GBSSI-YFP on starch granules diminished, while diffuse fluorescence appeared in the stroma and stromules (2 to 4 h, magenta arrowheads). Sometimes, SSGLs (white arrows) were observed in leaves exposed to darkness for 2 and 4 h. Yellow, GBSSI-YFP; red, chloroplasts.

(B) Enlarged area enclosed by a dashed line in **(A)** at 0 h.

(C) Enlarged area enclosed by a dashed line in **(A)** at 4 h.

(D) SSGLs appeared concurrently with stromules in leaves exposed to darkness for 2 or 4 h. Arrowheads indicate the stromules, while arrows refer to the SSGLs. One SSGL (cyan arrow) was in the stromule (cyan arrowhead). Bars = 10 μm.

(E) and **(F)** SSGLs could be sequestered in autophagosomes.

chloroplast-localized starch granule components are exported. Surprisingly, motile tubular structures extending from the chloroplast envelope were labeled by the released GBSSI-YFP (Figures 8C and 8D). These tubular extensions of chloroplasts were observed to extend, retract, blend, branch, and even bridge between two chloroplasts or two sides of a chloroplast (Figure 8A, 2 and 4 h; Figures 8C and 8D). We reasoned that these motile tubular structures were stromules (stroma-filled tubules) because they exhibited similar dynamic properties as those reported for stromules (Gunning, 2005). A fusion of the GBSSI transit peptide with enhanced YFP was used as a marker to visualize stromules (Shaw and Gray, 2011). Stromules are often observed in close proximity to other organelles (Kwok and Hanson, 2004b; Holzinger et al., 2007a, 2007b) and are suggested to have a role in transferring materials between compartments in the cell (Hanson and Sattarzadeh, 2011). Transportation of proteins as large as 550 kD between interconnected plastids had been reported (Kwok and Hanson, 2004a). An increased number of stromules was observed in the mesophyll cells of leaves exposed to darkness for 2 or 4 h (Figures 8A, 8C, and 8D). These stromules usually appeared simultaneously with the labeled round SSGLs but were markedly different from SSGLs in terms of morphology (Figure 8D). Stromules are usually 0.35 to 0.85 μm in diameter (Natesan et al., 2005). The stromules observed here had a diameter ranging from 0.4 to 1.2 μm, large enough to facilitate the passage of SSGLs (diameter of 0.5 μm). We sporadically detected SSGLs in the stromule (Figure 8D, cyan arrows). Furthermore, we performed an ultrastructural analysis of chloroplasts to confirm the presence of SSGLs in the stromule. We identified silver proteinate–stained SSGLs in the chloroplast protrusions lacking thylakoid membranes (Figure 10C), which are thought to be incipient or collapsed stromules (Hanson and Sattarzadeh, 2008). We did not observe SSGLs in the far-extending stromules because these stromules were extremely difficult to image in the thin TEM sections (Hanson and Sattarzadeh, 2008). Therefore, it is possible that SSGLs are exported from chloroplasts through stromules and then sequestered into the autophagic bodies for subsequent depletion.

The Autophagic Pathway Contributes Independently to Leaf Starch Degradation

Our studies suggest that autophagy contributes to leaf starch degradation besides the classic chloroplast pathway. How these two pathways cooperate is unclear. To investigate this, we designed a cosilencing assay in which both pathways were deficient. As a representative gene of the chloroplast pathway, *SEX1* is responsible for starch phosphorylation and its mutants exhibit the most severe starch-excess phenotype reported to date (Stettler et al., 2009). Among the autophagy-related genes tested in our study, silencing of *ATG6* resulted in the most starch accumulation in *N. benthamiana* plants (Figures 6 and 7). Therefore, we silenced *ATG6* and *SEX1* individually and simultaneously in *N. benthamiana* plants. Both the individual and combined silencing of *ATG6* and *SEX1* effectively reduced the corresponding mRNA levels and the silencing efficiency for each gene was similar in individually silenced and cosilenced plants (Figure 11B). We then determined the leaf starch contents by iodine staining and quantification assays, respectively. Excess starch was detected in both *ATG6*- and *SEX1*-silenced plants (Figures 11A and 11C). Moreover, the *ATG6*/*SEX1* cosilenced plants had a cumulative effect on starch accumulation (Figures 11A and 11C). Furthermore, in a prolonged dark treatment, both the *ATG6*- and *SEX1*-silenced leaves needed more time to destarch the reserved starch than the nonsilenced leaves, whereas the cosilenced leaves needed the most time (Figure 11D). These results suggest that both pathways contribute to leaf starch degradation and autophagy functions independently in this process.

Excessive Starch Is Accumulated in *Arabidopsis atg* Mutants

To investigate whether autophagy contributes to leaf starch in other plant species, we also analyzed the starch accumulation in *Arabidopsis atg* mutants. Two-week-old *atg2*, *atg5*, and *atg9* seedlings germinated on rich medium showed no significant difference in growth compared with wild-type Columbia seedlings (see Supplemental Figure 8A online). Quantitative analysis of the starch in the whole seedlings showed that the mutants accumulated more starch than did wild-type plants at the end of the night (see Supplemental Figure 8B online). Furthermore, we determined the leaf starch content of soil-grown *atg2*, *atg5*, and *atg9* mutants and observed a similar starch-excess phenotype (see Supplemental Figure 8D online). These results suggest that autophagy is involved in leaf starch depletion in *Arabidopsis*.

DISCUSSION

The Role of Autophagy in Leaf Starch Degradation

Glycogen, the analog of starch, is a form of polysaccharide widely used as an internal storage carbohydrate by Archaea, Bacteria, and Eukarya (Ball et al., 2011). Glycogen is selectively sequestered by autophagosomes and finally degraded in autolysosomes in a process named glycogen autophagy (Kotoulas et al., 2004). Glycogen autophagy in mammals has an indispensable

Figure 8. (continued).

(E) SSGLs labeled by GBSSI-YFP colocalized with autophagosomes labeled by CFP-ATG8f. Before dark treatment, SSGLs and autophagosomes were rarely observed in mesophyll cells (top panel). After a 4-h dark treatment, both SSGLs (white arrows) and autophagosomes (magenta arrows) appeared and some colocalized (magenta arrowheads; bottom panel). Bars = 10 μm.

(F) Time course of an autophagosome engulfing the SSGL and delivering it to the vacuole. The white arrowhead tracks the location of the SSGL within the autophagosome as it travels from the cytoplasm to the vacuole. Bars = 2 μm.

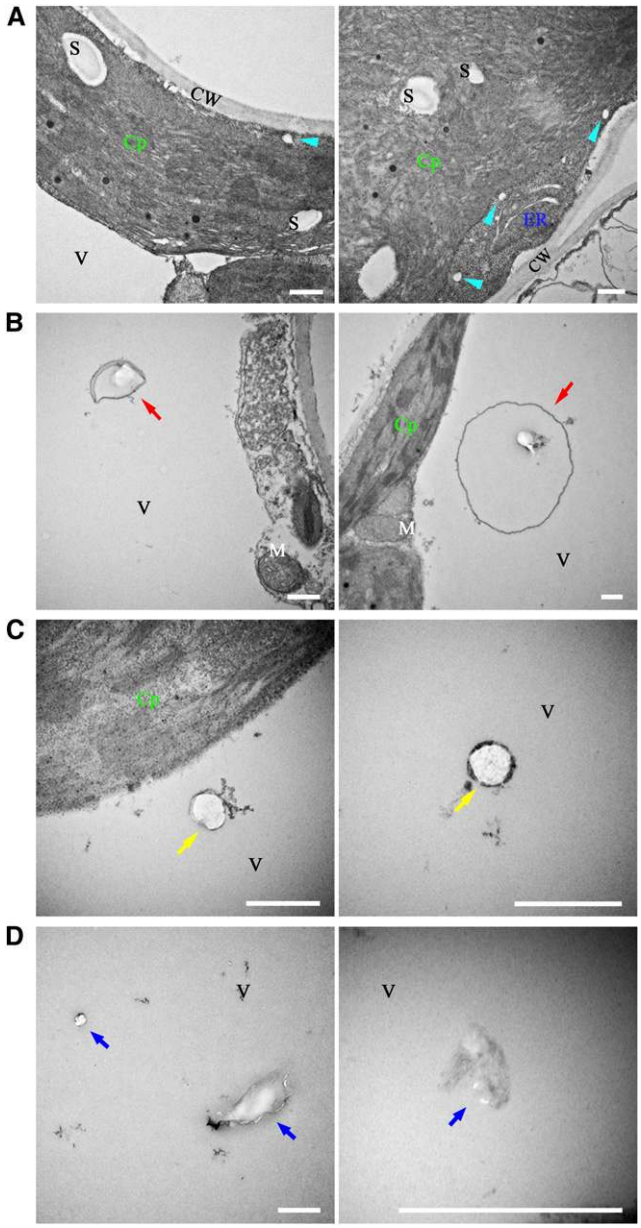

Figure 9. Ultrastructural Observation of SSGL Structures in the Cytoplasm and Vacuole.

(A) SSGLs in the cytoplasm. In leaves of plants exposed to darkness for 2 and 4 h, some SSGLs (cyan arrowheads) were observed in the cytoplasm in addition to the regular starch granules (S) located in the chloroplast. Note the boundary between the chloroplast and cytoplasm.
(B) to **(D)** SSGLs in the vacuole. In the same samples as mentioned above, SSGLs also appeared in the central vacuole. Three types of SSGLs were observed. The red arrows refer to SSGLs that were sequestered in single- or double-membrane vesicles **(B)**. The yellow arrows refer to SSGLs located directly in the vacuole **(C)**. The blue arrows refer to SSLGs that had almost completely degraded **(D)**.
Cp, chloroplast; CW, cell wall; ER, endoplasmic reticulum; M, mitochondrion; S, starch; V, vacuole. Bars = 500 nm.

role in helping newborns survive the immediate postnatal period by hydrolyzing storage glycogen and releasing massive amounts of Glc (Kotoulas et al., 2004). In plants, previous ultrastructural observations suggested that microautophagic machinery may be involved in the degradation of reserve starch (Toyooka et al., 2001). However, transitory starch degradation was thought to be confined to plastids (Zeeman et al., 2010), disputing the notion that plant leaf starch undergoes autophagic degradation. Here, we provide compelling evidence that autophagy, a non-plastidial pathway, contributes to transitory starch degradation. First, the expression of autophagy-related genes and autophagic activity in leaves was altered concurrently with nocturnal starch degradation. Second, SSGLs colocalized with autophagosomes. Third, SSGLs were observed in plant vacuoles. Fourth, disruption of autophagy reduced the number of vacuole-localized SSGLs. Fifth, blocking autophagy by the inhibitor 3-MA and silencing *ATG* genes resulted in a starch-excess phenotype.

Most *Arabidopsis* mutants lacking the genes involved in leaf starch degradation accumulated higher levels of starch, either in the day or at night (Zeeman et al., 1998a; Critchley et al., 2001;

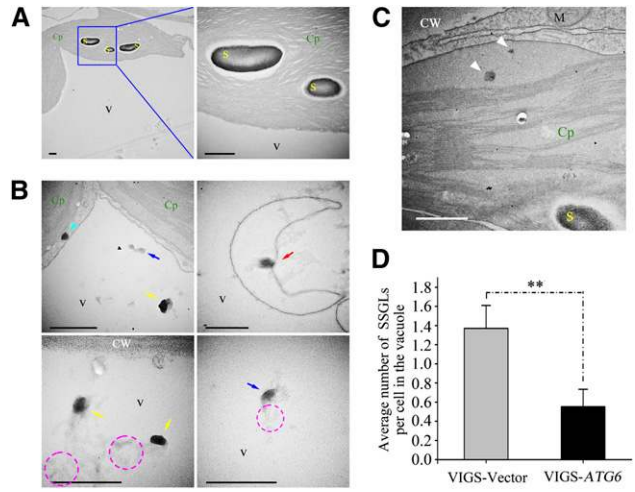

Figure 10. Ultrastructural Confirmation of the Starch Components in SSGLs by the Silver Proteinate Staining.

(A) Photographs of starch granules in the chloroplast stained by SP.
(B) Ultrastructural observation of SP-stained SSGLs in the cytoplasm (cyan arrowhead) and vacuole (arrows). The red, yellow, and blue arrows refer to SSGLs engulfed by a single-membrane vesicle, SSGLs located directly in the vacuole, and SSLGs that had almost completely degraded, respectively. In addition, some diffuse silver depositions with less intensity (representative areas enclosed by the magenta dashed lines) were often observed around the SSGLs.
(C) Image of SP-stained SSGLs (white arrowheads) deposited in a chloroplast protrusion that lacks thylakoid membranes.
(D) Quantification of the number of vacuole-localized SSGLs per cell in TEM images of *ATG6*-silenced and nonsilenced leaves exposed to darkness for 2 h. Values are means ± SE from 30 cells. Two asterisks indicate a significant difference ($P < 0.01$; Student's *t* test).
Cp, chloroplast; CW, cell wall; M, mitochondrion; S, starch; V, vacuole. Bars = 500 nm.

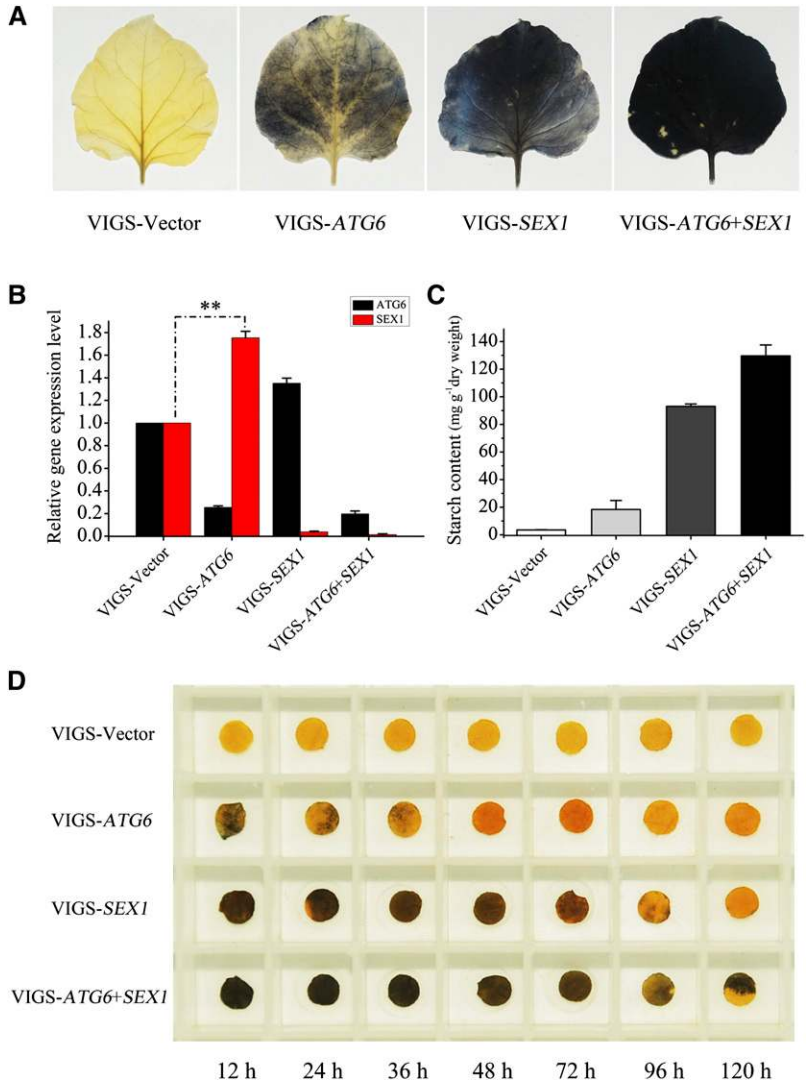

Figure 11. The Autophagic Pathway Contributes Independently to Leaf Starch Degradation.

(A) Iodine staining of the leaves from gene-silenced plants at the end of the night. Excess starch was detected in both *ATG6*-silenced and *SEX*-silenced leaves. Furthermore, more starch accumulated in the cosilenced leaves than in the individually silenced plants. The results were reproduced in three independent experiments using three leaves in each experiment. Representative results are presented.

(B) Relative gene expression in the gene-silenced plants. Real-time RT-PCR analysis showed no significant difference in the reduced expression levels between the individually silenced plants and cosilenced ones. Strikingly, increased expression of *SEX1* was detected in the *ATG6*-silenced leaves. Student's *t* test was applied to determine statistically significant differences (**$P < 0.01$).

(C) Quantification of leaf starch accumulated in the gene-silenced plants at the end of night. This assay showed similar results as those shown in **(A)**. Values are means ± SE from more than four replicate leaf samples.

(D) Iodine staining of leaf discs taken from a gene-silenced plant exposed to prolonged periods of darkness. The plants were kept in a dark room for as long as 120 h. More than three leaf discs were punched from the plants at a time point and incubated in ethanol to remove the leaf pigments. When all of the samples were harvested, they were stained with Lugol's solution. Representative results are presented.

[See online article for color version of this figure.]

Chia et al., 2004; Niittylä et al., 2004, 2006; Fulton et al., 2008; Comparot-Moss et al., 2010). We observed such starch-excess phenotypes when autophagy was blocked by an inhibitor or by silencing of autophagy-related genes in *N. benthamiana* (Figures 1, 6, and 7). Similar starch-excess phenotypes were observed in several *Arabidopsis atg* mutants (see Supplemental Figure 8 online). These results suggest that autophagy may contribute to leaf starch degradation in a range of plant species. The determined starch content in whole seedlings was higher than that in leaves at the end of the night (Figure 1B; see Supplemental Figure 8 online), since the starch in seedlings consisted of both transitory starch in leaves and reserve starch in the hypocotyl

and epicotyl (Figure 1A). Species-specific variations may exist in the effect of autophagy on starch degradation, since much less starch accumulated in the leaves of *Arabidopsis atg* mutants than in those of *N. benthamiana RNA interference* plants by the end of the night (see Supplemental Figure 8D online; Figures 6 and 7). Indeed, species-specific variations in the phenotypes of starch metabolism mutants and in starch levels during different development stages have been reported (Matheson and Wheatley, 1962; Geiger et al., 1995; Vriet et al., 2010; Graf and Smith, 2011).

Autophagy has been reported to play a role in nutrient recycling, and nitrogen or carbon deprivation triggers premature leaf senescence in *Arabidopsis atg* mutants (Doelling et al., 2002; Hanaoka et al., 2002; Thompson et al., 2005; Xiong et al., 2005; Patel and Dinesh-Kumar, 2008; Phillips et al., 2008; Chung et al., 2010). Nitrogen stress in plants restricted growth and altered starch metabolism (Rufty et al., 1988). However, nitrogen stress does not occur when plants are grown on rich medium or on nutrient-rich soil under the conditions used in our study. In addition, we did not observe any obvious growth defects in the 2-week-old *atg* mutant seedlings grown on rich MS medium (see Supplemental Figure 8A online), consistent with the finding that most nonlethal *atg* mutants show no difference in growth compared with the wild-type plants on nutrient-rich soil (Doelling et al., 2002; Hanaoka et al., 2002; Thompson et al., 2005; Xiong et al., 2005; Phillips et al., 2008). The 3-MA–treated *N. benthamiana* seedlings grown on rich medium showed reduced growth (see Supplemental Figure 1 online). Similar growth phenotypes were observed in the soil-grown *Arabidopsis atg2* and *atg5* mutants (see Supplemental Figure 8C online), consistent with previous reports (Yoshimoto et al., 2009; Wang et al., 2011). However, it is unlikely that these growth phenotypes are due to nutrient restriction, since all the *N. benthamiana* seedlings and *Arabidopsis atg* mutants are grown in nutrient-rich conditions. Furthermore, autophagy-deficient plants (*N. benthamiana* seedlings treated with 3-MA or *Arabidopsis atg* mutants) grown on rich medium still accumulated excess leaf starch (Figure 1; see Supplemental Figure 8B online). Therefore, the excess starch accumulation in autophagy-deficient plants is due to disruption of autophagy itself and not to possible nutrient limitation or poor plant growth.

Our studies suggest that both autophagy and the classic chloroplast pathway mediate leaf starch degradation. Crosstalk between the two pathways might exist because the leaf starch content of the cosilenced plants was more than the simple sum of the content in plants in which the two genes had been silenced individually (Figure 11C) and *ATG6*-silenced plants had higher *SEX1*-mRNA levels than the control (Figure 11B). We are unable to make a clear conclusion as to how much starch degradation occurs through each pathway due to the incomplete silencing caused by virus-induced gene silencing (VIGS). However, we found that the *SEX1*-silenced plants accumulate more starch than the *ATG6*-silenced plants (Figures 11A and 11C) and *SEX1*-silenced leaves needed more time to destarch than did the *ATG6*-silenced leaves in a prolonged dark treatment (Figure 11D). These results imply that the classic chloroplast pathway makes the larger contribution to leaf starch degradation.

Possible Mechanism Underlying Autophagic Degradation of Leaf Starch

In our study, we found that SSGLs are outside chloroplasts and sequestered in the autophagic bodies. These SSGLs were smaller (~0.5 μm in diameter) than normal starch granules (1 to 2 μm) in the chloroplasts (see Supplemental Figures 4B and 4C online). SSLGs were observed most readily in the leaves of plants exposed to darkness for 2 or 4 h (Figures 8D and 9). It is unclear how the SSGLs are generated. SSGLs may be produced from small portions of shrunken starch granules due to incomplete degradation. Fragmentation of the existing starch granules into small pieces during degradation may be another source of SSGLs because we observed fragmented granules in the silver proteinate-stained sections (see Supplemental Figure 9 online). The starch granule number per chloroplast at a given leaf age remained relatively constant in the diurnal cycle; accordingly, the initiation of starch granules is a strictly controlled event (Crumpton-Taylor et al., 2012). Thus, the overinitiated granules may also be exported in the form of SSGLs for degradation.

Our results suggest that SSGLs can be exported from chloroplasts. Thus, an exit channel would be needed for the SSGLs. Stromules, stroma-filled tubules that extend from the surface of plastids, may build bridges between chloroplasts and the cytoplasm and aid the export of SSGLs. Generally, stromules are scarce in mesophyll cells (Köhler and Hanson, 2000). However, we observed more stromules at the surface of plastids after exposure to darkness (Figure 8A), consistent with a previous report (Gray et al., 2012). These observations imply that stromules may be involved in nocturnal metabolism events, including starch depletion. Stromules usually appear concurrently with the SSGLs in leaves exposed to darkness (Figure 8D). The stromules observed in our study had a diameter of 0.4 to 1.2 μm, suggesting that they could accommodate SSGLs (0.5 μm in diameter). Indeed, we identified SSGLs in stromules (Figure 8D) and chloroplast protrusions (Figure 10C). These results suggest that SSGLs may be exported from chloroplasts through stromules. Under confocal microscopy, SSGLs were observed regularly at or around the chloroplast envelope (Figure 8). These SSGLs, which were similar to SSGLs observed in the cytoplasm by TEM (Figure 9A), were probably in the cytoplasm or were about to enter the cytoplasm. We still do not know how the SSGLs are released into the cytoplasm if stromules indeed function as the exit channel. The tip shedding or segmentation of stromules has been reported previously (Wildman et al., 1962; Gunning, 2005). SSGLs may be released into the cytoplasm from the tubule when the tip of stromules is shed as described (Gunning, 2005). Once released, SSGLs would be engulfed by autophagosomes and transported to the vacuole for further degradation (Figure 8F). Whether SSGLs are randomly or selectively sequestered in the autophagosomes is unknown.

The finding that autophagy contributes to leaf starch degradation suggests that some functional starch-degrading enzymes must be present inside vacuoles. Indeed, considerable β-amylase activity was detected in the vacuole of pea (*Pisum sativum*), wheat, and *Arabidopsis* (Ziegler and Beck, 1986; Lizotte et al., 1990; Monroe et al., 1991). Biochemical analysis showed that

β-amylase retained 70% of its maximal activity at pH levels of 4 to 5 (Lin et al., 1988). Furthermore, five of nine β-amylase proteins were predicted to be localized outside the chloroplast (Smith et al., 2004), and mutation of β-amylase 1, which is thought to be localized to the vacuole, has been reported to result in ~20% or almost complete loss of β-amylase activity in the leaves (Laby et al., 2001; Fulton et al., 2008). In addition, two α-amylases, AMY1 and AMY2, are extrachloroplastic (Yu et al., 2005). In this study, we identified SSGLs outside the chloroplast. This might solve the question as to whether extrachloroplastic substrates exist for amylases outside the chloroplast. However, it is still puzzling why mutation of some of the above-mentioned extrachloroplastic amylase genes has no obvious effect on leaf starch degradation (Yu et al., 2005; Fulton et al., 2008; Reinhold et al., 2011). It is possible that functional redundancy exists among these amylases or other unidentified starch-degrading enzymes occur in the vacuole.

Our results suggest that autophagy contributes to leaf starch degradation by directly engulfing SSGLs and transporting them into the vacuole. Autophagy may have additional indirect effects on starch depletion. The activities of enzymes involved in starch degradation are redox regulated, and these enzymes are active only in the reduced state (Mikkelsen et al., 2005; Sokolov et al., 2006; Sparla et al., 2006). Autophagy is involved in eliminating reactive oxygen species, and disruption of autophagy causes reactive oxygen species to accumulate (Xiong et al., 2007; Yoshimoto et al., 2009). Thus, autophagy might influence starch degradation indirectly by affecting the redox regulation of the enzymes that catalyze this process.

METHODS

Plant Materials and Growth Conditions

Nicotiana benthamiana plants were cultivated in pots placed in growth rooms at 25°C under a 16-h-light/8-h-dark cycle, unless otherwise stated. *Arabidopsis thaliana atg* mutants were described previously (Wang et al., 2011). Wild-type *Arabidopsis* plants and mutants in the Columbia background were grown in controlled environment chambers under a 16-h-light/8-h-dark cycle with 60% relative humidity at 22°C. Light intensity was 100 μmol photons m^{-2} s^{-1} unless otherwise stated. Starch content was determined in 6-week-old plants.

Plasmids

VIGS vectors pTRV1, pTRV2, pTRV2-*ATG6*, pTRV2-*PI3K*/*VPS34*, pTRV2-*ATG3*, and pTRV2-*ATG7* were described previously (Liu et al., 2002, 2005). pTRV2-*ATG2*, pTRV2-*ATG5*, and pTRV2-*VTI12* were constructed by cloning the respective cDNA fragments into pTRV2. To generate VIGS vectors for the cosilencing assay, we inserted the equal length of DNA fragment into TRV VIGS vector by fusing the target DNA fragment with a nonhost DNA fragment to obtain similar gene silencing efficiency. For example, in the construct used for cosilencing *ATG6* and *SEX1*, we fused a 450-bp sequence of *ATG6* with a 450-bp sequence of *SEX1*, while in the constructs used for single-gene silencing, we fused the same 450-bp sequence of *ATG6* or *SEX1* with a 450-bp sequence of a nonhost gene, luciferase.

DNA fragments of CFP-ATG8f and GBSSI-YFP were obtained by overlapping PCR. Primers used for overlapping PCR are listed in Supplemental Table 1 online. The resulting PCR products were cloned between the duplicated 35S cauliflower mosaic virus promoter and Nos terminator of pJG045, a pCAMBIA1300-based T-DNA vector (Zhao et al., 2013).

VIGS Assay

For the VIGS assay, the above-mentioned tobacco rattle virus (TRV) vectors were introduced into *Agrobacterium tumefaciens* strain GV3101. *Agrobacterium* containing TRV1 or TRV2 derivative plasmids was grown overnight on a 28°C shaker. *Agrobacterium* harboring TRV1 or TRV2 derivative vectors was resuspended in infiltration buffer (10 mM $MgCl_2$, 10 mM MES, and 200 μM acetosyringone) and mixed at a 1:1 ratio. After a 4-h incubation at room temperature, the mixed *Agrobacterium* cultures were infiltrated into the leaves of six-leaf stage *N. benthamiana* plants. A silenced phenotype appeared in the upper leaves at ~2 weeks post infiltration.

Iodine Staining and Starch Content Measurement

Detached leaves were boiled in 95% ethanol to remove leaf pigments thoroughly and then washed twice with deionized water. Rehydrated leaves were stained for 10 min in 5% Lugol's solution (5% [w/v] I_2 and 10% [w/v] KI) and incubated in water to allow fading until a clear background was obtained. Iodine staining was repeated at least three times for each construct.

For starch quantification, leaves decolorized by ethanol were dried, frozen in liquid N_2, and homogenized into powder using a mortar and pestle. Starch content was subsequently measured using a starch assay kit (Sigma-Aldrich; product code STA20).

Treatment of Plants by Autophagy Inhibitor

For the seedling assay, surface-sterilized seeds were plated directly on the MS plates with or without 5 mM 3-MA and grown under normal long-day conditions for 2 weeks. Samples were harvested at the end of the day or night and subjected to iodine staining.

RT-PCR Analysis

Total RNAs were extracted using Trizol reagent (Tiangen) from the leaf samples and treated with RNase-free DNase I (Sigma-Aldrich) to remove potential DNA contamination. Isolated RNA was reverse transcribed using oligo(dT) primer and TRANScript moloney murine leukemia virus reverse transcriptase according to the manufacturer's manual (Tiangen).

For the *ATG* gene expression analysis, real-time PCR was performed on a Bio-Rad CFX96 real-time PCR detection system using Power SYBR Green PCR master mix (Applied Biosystems). To confirm the silencing of *ATG* genes in individual *N. benthamiana* plants, RT-PCR was performed as described previously (Liu et al., 2004). *EF1A* was used as the internal control. Primers used for RT-PCR analysis are listed in Supplemental Table 1 online.

Confocal Microscopy

N. benthamiana plants grown in pots under normal 16-h-light/8-h-dark conditions were subjected to complete darkness for 0, 2, 4, and 8 h. Leaf samples were excised from individual plants exposed to different periods of darkness and monitored by confocal microscopy. Confocal images were acquired using an inverted Zeiss LSM 710 laser scanning microscope.

For MDC staining, the leaves were infiltrated with 100 μM E-64d (Sigma-Aldrich) to ensure that the samples were treated with E-64d for 8 to 10 h. After the dark treatment, the E-64d–infiltrated parts of the leaves

were excised and immediately vacuum infiltrated with 50 μM MDC (Sigma-Aldrich) for 10 min, followed by two washes with PBS buffer. MDC-incorporated structures were excited by a wavelength of 405 nm and detected at 400 to 580 nm. Chloroplast autofluorescence was excited at 543 nm and detected at 580 to 695 nm.

To observe autophagosomes using the autophagy marker CFP-ATG8f, *Agrobacterium* harboring CFP-ATG8f was cultured, harvested, and resuspended in infiltration buffer (10 mM $MgCl_2$, 10 mM MES, and 200 μM acetosyringone) and infiltrated into leaves of six-leaf stage *N. benthamiana* plants. Two days after agroinfiltration, the samples underwent additional infiltration with the protease inhibitor concanamycin A (1 μM) to ensure that the samples were exposed to concanamycin treatment for 8 h. Leaves were then excised after the dark treatment, incubated in PBS buffer, and monitored using a Zeiss LSM 710 with an excitation light of 405 nm.

Starch granules labeled with GBSSI-YFP were monitored by a 514-nm excitation laser.

TEM

Excised leaf discs were immediately cut into small pieces (~1 mm × 2 mm) and fixed with 2.5% glutaraldehyde in 0.1 M PBS, pH 6.8, for 12 h. After washing with PBS buffer, the samples were fixed with 1% OsO_4 at room temperature for 2 h, dehydrated in a graded series of ethanol, and then embedded in Epon 812. Ultrathin (70-nm) sections were prepared on an ultramicrotome (Leica EM UC6) with a diamond knife and collected on Formvar-coated grids. Subsequently, sections were stained with uranyl acetate and lead citrate and examined with an electron microscope (Hitachi H-7650). For PA-TCH-SP staining of starch, we made some modifications to the protocol described by Thiery (1967). The sections were collected on gold grids and incubated as follows: 1% PA (Sigma-Aldrich), 30 min; twice-distilled water, 3 × 10 min; 1% TCH (Sigma-Aldrich) in 10% acetic acid, in darkness for 6 h; 10% acetic acid, 10 min; 5% acetic acid, 10 min; 2% acetic acid, 10 min; twice-distilled water, 2 × 15 min; 1% SP (Sigma-Aldrich), 50°C, 30 min in darkness; and twice-distilled water, 2 × 15 min. The stained sections were kept in darkness until they were examined. To exclude the possibility of unspecific staining, several control treatments (TCH-SP, PA-SP, and SP) were performed by omitting one or two steps of the standard PA-TCH-SP method as described (Courtoy and Simar, 1974).

Accession Numbers

Sequence data from this article can be found in the GenBank/EMBL data libraries under the following accession numbers: tobacco (*Nicotiana tabacum*) *ATG2* (JX175262), *N. benthamiana ATG5* (JX175258), *N. benthamiana VTI12* (JX232203), *N. tabacum ATG8*f (JX175260), and *N. tabacum GBSSI* (JX175261).

Supplemental Data

The following materials are available in the online version of this article.

Supplemental Figure 1. 3-MA Treatment Reduces the Growth of Seedlings.

Supplemental Figure 2. Reduced Expression Levels of *ATG* Genes in the Silenced Plants.

Supplemental Figure 3. Autophagosomes Are Rarely Observed in *ATG6*-Silenced Plants Imaged by Confocal Laser Scanning Microscopy.

Supplemental Figure 4. Characterization of Starch Granules and SSGLs.

Supplemental Figure 5. The Starch-Excess Phenotype in *ATG6*-Silenced Plants Is Due to the Reduced Starch Degradation during the Night.

Supplemental Figure 6. Autophagosome Formation Is Reduced in Other *ATG*-Silenced Plants Examined by Confocal Laser Scanning Microscopy.

Supplemental Figure 7. Ultrastructural Analysis of Silver Proteinate–Stained SSGLs in the Vacuole.

Supplemental Figure 8. Developmental Phenotypes and Leaf Starch Content in Wild-Type *Arabidopsis* and *atg* Mutants.

Supplemental Figure 9. Ultrastructure of Fragmented Starch Granules in Leaves Exposed to Darkness.

Supplemental Table 1. List of Primers Used in This Study.

ACKNOWLEDGMENTS

This work was supported by the National Basic Research Program of China (Grant 2011CB910100) and the National Natural Science Foundation of China (Grants 30930060 and 31071169).

AUTHOR CONTRIBUTIONS

Yu.L. and Y.W. initiated the project, designed the experiments, and wrote the article. Y.W., B.Y., J.Z., J.G., Yi.L., S.H., L.H., and Y.D. performed the research. Yu.L., Y.W., and B.Y. analyzed the data. Y.H. and D.T. discussed and revised the article.

Received December 24, 2012; revised March 12, 2013; accepted March 20, 2013; published April 19, 2013.

REFERENCES

Aubert, S., Gout, E., Bligny, R., Marty-Mazars, D., Barrieu, F., Alabouvette, J., Marty, F., and Douce, R. (1996). Ultrastructural and biochemical characterization of autophagy in higher plant cells subjected to carbon deprivation: Control by the supply of mitochondria with respiratory substrates. J. Cell Biol. **133:** 1251–1263.

Bahaji, A., Li, J., Ovecka, M., Ezquer, I., Muñoz, F.J., Baroja-Fernández, E., Romero, J.M., Almagro, G., Montero, M., Hidalgo, M., Sesma, M.T., and Pozueta-Romero, J. (2011). *Arabidopsis thaliana* mutants lacking ADP-glucose pyrophosphorylase accumulate starch and wild-type ADP-glucose content: further evidence for the occurrence of important sources, other than ADP-glucose pyrophosphorylase, of ADP-glucose linked to leaf starch biosynthesis. Plant Cell Physiol. **52:** 1162–1176.

Ball, S., Colleoni, C., Cenci, U., Raj, J.N., and Tirtiaux, C. (2011). The evolution of glycogen and starch metabolism in eukaryotes gives molecular clues to understand the establishment of plastid endosymbiosis. J. Exp. Bot. **62:** 1775–1801.

Baunsgaard, L., Lütken, H., Mikkelsen, R., Glaring, M.A., Pham, T.T., and Blennow, A. (2005). A novel isoform of glucan, water dikinase phosphorylates pre-phosphorylated alpha-glucans and is involved in starch degradation in *Arabidopsis*. Plant J. **41:** 595–605.

Biederbick, A., Kern, H.F., and Elsässer, H.P. (1995). Monodansylcadaverine (MDC) is a specific in vivo marker for autophagic vacuoles. Eur. J. Cell Biol. **66:** 3–14.

Blommaart, E.F., Krause, U., Schellens, J.P., Vreeling-Sindelárová, H., and Meijer, A.J. (1997). The phosphatidylinositol 3-kinase inhibitors wortmannin and LY294002 inhibit autophagy in isolated rat hepatocytes. Eur. J. Biochem. **243:** 240–246.

Braña, A.F., Manzanal, M.B., and Hardisson, C. (1980). Occurrence of polysaccharide granules in sporulating hyphae of *Streptomyces viridochromogenes*. J. Bacteriol. **144:** 1139–1142.

Chia, T., Thorneycroft, D., Chapple, A., Messerli, G., Chen, J., Zeeman, S.C., Smith, S.M., and Smith, A.M. (2004). A cytosolic glucosyltransferase is required for conversion of starch to sucrose in *Arabidopsis* leaves at night. Plant J. **37:** 853–863.

Cho, M.H., Lim, H., Shin, D.H., Jeon, J.S., Bhoo, S.H., Park, Y.I., and Hahn, T.R. (December 22, 2010). Role of the plastidic glucose translocator in the export of starch degradation products from the chloroplasts in *Arabidopsis thaliana*. New Phytol. http://dx.doi.org/10.1111/j.1469-8137.2010.03580.x.

Chung, T., Phillips, A.R., and Vierstra, R.D. (2010). ATG8 lipidation and ATG8-mediated autophagy in *Arabidopsis* require ATG12 expressed from the differentially controlled ATG12A AND ATG12B loci. Plant J. **62:** 483–493.

Comparot-Moss, S., et al. (2010). A putative phosphatase, LSF1, is required for normal starch turnover in *Arabidopsis* leaves. Plant Physiol. **152:** 685–697.

Contento, A.L., Xiong, Y., and Bassham, D.C. (2005). Visualization of autophagy in *Arabidopsis* using the fluorescent dye monodansylcadaverine and a GFP-AtATG8e fusion protein. Plant J. **42:** 598–608.

Courtoy, R., and Simar, L.J. (1974). Importance of controls for the demonstration of carbohydrates in electron microscopy with the silver methenamine or the thiocarbohydrazide-silver proteinate methods. J. Microsc. **100:** 199–211.

Critchley, J.H., Zeeman, S.C., Takaha, T., Smith, A.M., and Smith, S.M. (2001). A critical role for disproportionating enzyme in starch breakdown is revealed by a knock-out mutation in *Arabidopsis*. Plant J. **26:** 89–100.

Crumpton-Taylor, M., Grandison, S., Png, K.M., Bushby, A.J., and Smith, A.M. (2012). Control of starch granule numbers in *Arabidopsis* chloroplasts. Plant Physiol. **158:** 905–916.

Delatte, T., Umhang, M., Trevisan, M., Eicke, S., Thorneycroft, D., Smith, S.M., and Zeeman, S.C. (2006). Evidence for distinct mechanisms of starch granule breakdown in plants. J. Biol. Chem. **281:** 12050–12059.

Doelling, J.H., Walker, J.M., Friedman, E.M., Thompson, A.R., and Vierstra, R.D. (2002). The APG8/12-activating enzyme APG7 is required for proper nutrient recycling and senescence in *Arabidopsis thaliana*. J. Biol. Chem. **277:** 33105–33114.

Fettke, J., Hejazi, M., Smirnova, J., Höchel, E., Stage, M., and Steup, M. (2009). Eukaryotic starch degradation: Integration of plastidial and cytosolic pathways. J. Exp. Bot. **60:** 2907–2922.

Fulton, D.C., et al. (2008). Beta-AMYLASE4, a noncatalytic protein required for starch breakdown, acts upstream of three active beta-amylases in *Arabidopsis* chloroplasts. Plant Cell **20:** 1040–1058.

Geiger, D.R., Shieh, W.J., and Yu, X.M. (1995). Photosynthetic carbon metabolism and translocation in wild-type and starch-deficient mutant *Nicotiana sylvestris* L. Plant Physiol. **107:** 507–514.

Ghiglione, H.O., Gonzalez, F.G., Serrago, R., Maldonado, S.B., Chilcott, C., Curá, J.A., Miralles, D.J., Zhu, T., and Casal, J.J. (2008). Autophagy regulated by day length determines the number of fertile florets in wheat. Plant J. **55:** 1010–1024.

Graf, A., and Smith, A.M. (2011). Starch and the clock: The dark side of plant productivity. Trends Plant Sci. **16:** 169–175.

Gray, J.C., Hansen, M.R., Shaw, D.J., Graham, K., Dale, R., Smallman, P., Natesan, S.K., and Newell, C.A. (2012). Plastid stromules are induced by stress treatments acting through abscisic acid. Plant J. **69:** 387–398.

Gunning, B.E. (2005). Plastid stromules: Video microscopy of their outgrowth, retraction, tensioning, anchoring, branching, bridging, and tip-shedding. Protoplasma **225:** 33–42.

Han, S., Yu, B., Wang, Y., and Liu, Y. (2011). Role of plant autophagy in stress response. Protein Cell **2:** 784–791.

Hanaoka, H., Noda, T., Shirano, Y., Kato, T., Hayashi, H., Shibata, D., Tabata, S., and Ohsumi, Y. (2002). Leaf senescence and starvation-induced chlorosis are accelerated by the disruption of an *Arabidopsis* autophagy gene. Plant Physiol. **129:** 1181–1193.

Hanson, M.R., and Sattarzadeh, A. (2008). Dynamic morphology of plastids and stromules in angiosperm plants. Plant Cell Environ. **31:** 646–657.

Hanson, M.R., and Sattarzadeh, A. (2011). Stromules: Recent insights into a long neglected feature of plastid morphology and function. Plant Physiol. **155:** 1486–1492.

Hofius, D., Munch, D., Bressendorff, S., Mundy, J., and Petersen, M. (2011). Role of autophagy in disease resistance and hypersensitive response-associated cell death. Cell Death Differ. **18:** 1257–1262.

Holzinger, A., Buchner, O., Lütz, C., and Hanson, M.R. (2007a). Temperature-sensitive formation of chloroplast protrusions and stromules in mesophyll cells of *Arabidopsis thaliana*. Protoplasma **230:** 23–30.

Holzinger, A., Wasteneys, G.O., and Lütz, C. (2007b). Investigating cytoskeletal function in chloroplast protrusion formation in the arctic-alpine plant *Oxyria digyna*. Plant Biol. (Stuttg.) **9:** 400–410.

Inoue, Y., Suzuki, T., Hattori, M., Yoshimoto, K., Ohsumi, Y., and Moriyasu, Y. (2006). AtATG genes, homologs of yeast autophagy genes, are involved in constitutive autophagy in Arabidopsis root tip cells. Plant Cell Physiol. **47:** 1641–1652.

Ishida, H., Yoshimoto, K., Izumi, M., Reisen, D., Yano, Y., Makino, A., Ohsumi, Y., Hanson, M.R., and Mae, T. (2008). Mobilization of rubisco and stroma-localized fluorescent proteins of chloroplasts to the vacuole by an ATG gene-dependent autophagic process. Plant Physiol. **148:** 142–155.

Izumi, M., Wada, S., Makino, A., and Ishida, H. (2010). The autophagic degradation of chloroplasts via rubisco-containing bodies is specifically linked to leaf carbon status but not nitrogen status in *Arabidopsis*. Plant Physiol. **154:** 1196–1209.

Kaplan, F., and Guy, C.L. (2005). RNA interference of *Arabidopsis* beta-amylase8 prevents maltose accumulation upon cold shock and increases sensitivity of PSII photochemical efficiency to freezing stress. Plant J. **44:** 730–743.

Klionsky, D.J., and Emr, S.D. (2000). Autophagy as a regulated pathway of cellular degradation. Science **290:** 1717–1721.

Köhler, R.H., and Hanson, M.R. (2000). Plastid tubules of higher plants are tissue-specific and developmentally regulated. J. Cell Sci. **113:** 81–89.

Kotoulas, O.B., Kalamidas, S.A., and Kondomerkos, D.J. (2004). Glycogen autophagy. Microsc. Res. Tech. **64:** 10–20.

Kötting, O., Pusch, K., Tiessen, A., Geigenberger, P., Steup, M., and Ritte, G. (2005). Identification of a novel enzyme required for starch metabolism in *Arabidopsis* leaves. The phosphoglucan, water dikinase. Plant Physiol. **137:** 242–252.

Kötting, O., Santelia, D., Edner, C., Eicke, S., Marthaler, T., Gentry, M.S., Comparot-Moss, S., Chen, J., Smith, A.M., Steup, M., Ritte, G., and Zeeman, S.C. (2009). STARCH-EXCESS4 is a laforin-like Phosphoglucan phosphatase required for starch degradation in *Arabidopsis thaliana*. Plant Cell **21:** 334–346.

Kwok, E.Y., and Hanson, M.R. (2004a). GFP-labelled Rubisco and aspartate aminotransferase are present in plastid stromules and traffic between plastids. J. Exp. Bot. **55:** 595–604.

Kwok, E.Y., and Hanson, M.R. (2004b). Plastids and stromules interact with the nucleus and cell membrane in vascular plants. Plant Cell Rep. **23:** 188–195.

Kwon, S.I., Cho, H.J., Jung, J.H., Yoshimoto, K., Shirasu, K., and Park, O.K. (2010). The Rab GTPase RabG3b functions in autophagy

and contributes to tracheary element differentiation in *Arabidopsis*. Plant J. **64:** 151–164.

Laby, R.J., Kim, D., and Gibson, S.I. (2001). The ram1 mutant of *Arabidopsis* exhibits severely decreased beta-amylase activity. Plant Physiol. **127:** 1798–1807.

Lai, Z., Wang, F., Zheng, Z., Fan, B., and Chen, Z. (2011). A critical role of autophagy in plant resistance to necrotrophic fungal pathogens. Plant J. **66:** 953–968.

Lenz, H.D., et al. (2011). Autophagy differentially controls plant basal immunity to biotrophic and necrotrophic pathogens. Plant J. **66:** 818–830.

Levine, B., and Klionsky, D.J. (2004). Development by self-digestion: Molecular mechanisms and biological functions of autophagy. Dev. Cell **6:** 463–477.

Lin, T.P., Spilatro, S.R., and Preiss, J. (1988). Subcellular localization and characterization of amylases in Arabidopsis leaf. Plant Physiol. **86:** 251–259.

Liu, Y., Burch-Smith, T., Schiff, M., Feng, S., and Dinesh-Kumar, S. P. (2004). Molecular chaperone Hsp90 associates with resistance protein N and its signaling proteins SGT1 and Rar1 to modulate an innate immune response in plants. J. Biol. Chem. **279:** 2101–2108.

Liu, Y., Schiff, M., Czymmek, K., Tallóczy, Z., Levine, B., and Dinesh-Kumar, S.P. (2005). Autophagy regulates programmed cell death during the plant innate immune response. Cell **121:** 567–577.

Liu, Y., Schiff, M., and Dinesh-Kumar, S.P. (2002). Virus-induced gene silencing in tomato. Plant J. **31:** 777–786.

Liu, Y., Xiong, Y., and Bassham, D.C. (2009). Autophagy is required for tolerance of drought and salt stress in plants. Autophagy **5:** 954–963.

Lizotte, P.A., Henson, C.A., and Duke, S.H. (1990). Purification and characterization of pea epicotyl beta-amylase. Plant Physiol. **92:** 615–621.

Lo, H.K., Malinin, T.I., and Malinin, G.I. (1987). A modified periodic acid-thiocarbohydrazide-silver proteinate staining sequence for enhanced contrast and resolution of glycogen depositions by transmission electron microscopy. J. Histochem. Cytochem. **35:** 393–399.

Massey, A., Kiffin, R., and Cuervo, A.M. (2004). Pathophysiology of chaperone-mediated autophagy. Int. J. Biochem. Cell Biol. **36:** 2420–2434.

Matheson, N.K., and Wheatley, J.M. (1962). Starch changes in developing and senescing tobacco leaves. Aust. J. Biol. Sci. **15:** 445–458.

Mikkelsen, R., Mutenda, K.E., Mant, A., Schürmann, P., and Blennow, A. (2005). Alpha-glucan, water dikinase (GWD): A plastidic enzyme with redox-regulated and coordinated catalytic activity and binding affinity. Proc. Natl. Acad. Sci. USA **102:** 1785–1790.

Mizushima, N., Yoshimori, T., and Ohsumi, Y. (2011). The role of Atg proteins in autophagosome formation. Annu. Rev. Cell Dev. Biol. **27:** 107–132.

Monroe, J.D., Salminen, M.D., and Preiss, J. (1991). Nucleotide sequence of a cDNA clone encoding a beta-amylase from *Arabidopsis thaliana*. Plant Physiol. **97:** 1599–1601.

Moriyasu, Y., and Ohsumi, Y. (1996). Autophagy in tobacco suspension-cultured cells in response to sucrose starvation. Plant Physiol. **111:** 1233–1241.

Munafó, D.B., and Colombo, M.I. (2001). A novel assay to study autophagy: Regulation of autophagosome vacuole size by amino acid deprivation. J. Cell Sci. **114:** 3619–3629.

Natesan, S.K., Sullivan, J.A., and Gray, J.C. (2005). Stromules: A characteristic cell-specific feature of plastid morphology. J. Exp. Bot. **56:** 787–797.

Niittylä, T., Comparot-Moss, S., Lue, W.L., Messerli, G., Trevisan, M., Seymour, M.D., Gatehouse, J.A., Villadsen, D., Smith, S.M., Chen, J., Zeeman, S.C., and Smith, A.M. (2006). Similar protein phosphatases control starch metabolism in plants and glycogen metabolism in mammals. J. Biol. Chem. **281:** 11815–11818.

Niittylä, T., Messerli, G., Trevisan, M., Chen, J., Smith, A.M., and Zeeman, S.C. (2004). A previously unknown maltose transporter essential for starch degradation in leaves. Science **303:** 87–89.

Patel, S., and Dinesh-Kumar, S.P. (2008). *Arabidopsis* ATG6 is required to limit the pathogen-associated cell death response. Autophagy **4:** 20–27.

Phillips, A.R., Suttangkakul, A., and Vierstra, R.D. (2008). The ATG12-conjugating enzyme ATG10 is essential for autophagic vesicle formation in *Arabidopsis thaliana*. Genetics **178:** 1339–1353.

Reinhold, H., Soyk, S., Simková, K., Hostettler, C., Marafino, J., Mainiero, S., Vaughan, C.K., Monroe, J.D., and Zeeman, S.C. (2011). β-Amylase-like proteins function as transcription factors in *Arabidopsis*, controlling shoot growth and development. Plant Cell **23:** 1391–1403.

Ritte, G., Heydenreich, M., Mahlow, S., Haebel, S., Kötting, O., and Steup, M. (2006). Phosphorylation of C6- and C3-positions of glucosyl residues in starch is catalysed by distinct dikinases. FEBS Lett. **580:** 4872–4876.

Rufty, T.W., Huber, S.C., and Volk, R.J. (1988). Alterations in leaf carbohydrate metabolism in response to nitrogen stress. Plant Physiol. **88:** 725–730.

Santelia, D., and Zeeman, S.C. (2011). Progress in *Arabidopsis* starch research and potential biotechnological applications. Curr. Opin. Biotechnol. **22:** 271–280.

Seglen, P.O., and Gordon, P.B. (1982). 3-Methyladenine: Specific inhibitor of autophagic/lysosomal protein degradation in isolated rat hepatocytes. Proc. Natl. Acad. Sci. USA **79:** 1889–1892.

Shaw, D.J., and Gray, J.C. (2011). Visualisation of stromules in transgenic wheat expressing a plastid-targeted yellow fluorescent protein. Planta **233:** 961–970.

Smith, S.M., Fulton, D.C., Chia, T., Thorneycroft, D., Chapple, A., Dunstan, H., Hylton, C., Zeeman, S.C., and Smith, A.M. (2004). Diurnal changes in the transcriptome encoding enzymes of starch metabolism provide evidence for both transcriptional and posttranscriptional regulation of starch metabolism in *Arabidopsis* leaves. Plant Physiol. **136:** 2687–2699.

Sokolov, L.N., Dominguez-Solis, J.R., Allary, A.L., Buchanan, B.B., and Luan, S. (2006). A redox-regulated chloroplast protein phosphatase binds to starch diurnally and functions in its accumulation. Proc. Natl. Acad. Sci. USA **103:** 9732–9737.

Sparla, F., Costa, A., Lo Schiavo, F., Pupillo, P., and Trost, P. (2006). Redox regulation of a novel plastid-targeted beta-amylase of *Arabidopsis*. Plant Physiol. **141:** 840–850.

Stettler, M., Eicke, S., Mettler, T., Messerli, G., Hörtensteiner, S., and Zeeman, S.C. (2009). Blocking the metabolism of starch breakdown products in *Arabidopsis* leaves triggers chloroplast degradation. Mol. Plant **2:** 1233–1246.

Szydlowski, N., et al. (2009). Starch granule initiation in *Arabidopsis* requires the presence of either class IV or class III starch synthases. Plant Cell **21:** 2443–2457.

Takatsuka, C., Inoue, Y., Matsuoka, K., and Moriyasu, Y. (2004). 3-Methyladenine inhibits autophagy in tobacco culture cells under sucrose starvation conditions. Plant Cell Physiol. **45:** 265–274.

Thiery, J. (1967). Mise en évidence des polysaccharides sur coupes fines en microscopie électronique. J. Microsc. (Paris) **6:** 987–1018.

Thompson, A.R., Doelling, J.H., Suttangkakul, A., and Vierstra, R.D. (2005). Autophagic nutrient recycling in *Arabidopsis* directed

by the ATG8 and ATG12 conjugation pathways. Plant Physiol. **138:** 2097–2110.

Toyooka, K., Okamoto, T., and Minamikawa, T. (2001). Cotyledon cells of *Vigna mungo* seedlings use at least two distinct autophagic machineries for degradation of starch granules and cellular components. J. Cell Biol. **154:** 973–982.

Vriet, C., Welham, T., Brachmann, A., Pike, M., Pike, J., Perry, J., Parniske, M., Sato, S., Tabata, S., Smith, A.M., and Wang, T.L. (2010). A suite of *Lotus japonicus* starch mutants reveals both conserved and novel features of starch metabolism. Plant Physiol. **154:** 643–655.

Wada, S., Ishida, H., Izumi, M., Yoshimoto, K., Ohsumi, Y., Mae, T., and Makino, A. (2009). Autophagy plays a role in chloroplast degradation during senescence in individually darkened leaves. Plant Physiol. **149:** 885–893.

Wang, Y., Nishimura, M.T., Zhao, T., and Tang, D. (2011). ATG2, an autophagy-related protein, negatively affects powdery mildew resistance and mildew-induced cell death in *Arabidopsis*. Plant J. **68:** 74–87.

Wattebled, F., Dong, Y., Dumez, S., Delvallé, D., Planchot, V., Berbezy, P., Vyas, D., Colonna, P., Chatterjee, M., Ball, S., and D'Hulst, C. (2005). Mutants of *Arabidopsis* lacking a chloroplastic isoamylase accumulate phytoglycogen and an abnormal form of amylopectin. Plant Physiol. **138:** 184–195.

Wildman, S.G., Hongladarom, T., and Honda, S.I. (1962). Chloroplasts and mitochondria in living plant cells: Cinephotomicrographic studies. Science **138:** 434–436.

Xie, Z., and Klionsky, D.J. (2007). Autophagosome formation: Core machinery and adaptations. Nat. Cell Biol. **9:** 1102–1109.

Xiong, Y., Contento, A.L., and Bassham, D.C. (2005). AtATG18a is required for the formation of autophagosomes during nutrient stress and senescence in *Arabidopsis thaliana*. Plant J. **42:** 535–546.

Xiong, Y., Contento, A.L., Nguyen, P.Q., and Bassham, D.C. (2007). Degradation of oxidized proteins by autophagy during oxidative stress in *Arabidopsis*. Plant Physiol. **143:** 291–299.

Yano, K., Suzuki, T., and Moriyasu, Y. (2007). Constitutive autophagy in plant root cells. Autophagy **3:** 360–362.

Yoshikawa, H., Morioka, H., and Yoshida, Y. (1988). Ultrastructural detection of carbohydrates in the pellicle of *Pneumocystis carinii*. Parasitol. Res. **74:** 537–543.

Yoshimoto, K., Hanaoka, H., Sato, S., Kato, T., Tabata, S., Noda, T., and Ohsumi, Y. (2004). Processing of ATG8s, ubiquitin-like proteins, and their deconjugation by ATG4s are essential for plant autophagy. Plant Cell **16:** 2967–2983.

Yoshimoto, K., Jikumaru, Y., Kamiya, Y., Kusano, M., Consonni, C., Panstruga, R., Ohsumi, Y., and Shirasu, K. (2009). Autophagy negatively regulates cell death by controlling NPR1-dependent salicylic acid signaling during senescence and the innate immune response in *Arabidopsis*. Plant Cell **21:** 2914–2927.

Yu, T.S., et al. (2001). The *Arabidopsis* sex1 mutant is defective in the R1 protein, a general regulator of starch degradation in plants, and not in the chloroplast hexose transporter. Plant Cell **13:** 1907–1918.

Yu, T.S., et al. (2005). α-Amylase is not required for breakdown of transitory starch in *Arabidopsis* leaves. J. Biol. Chem. **280:** 9773–9779.

Zeeman, S.C., Kossmann, J., and Smith, A.M. (2010). Starch: Its metabolism, evolution, and biotechnological modification in plants. Annu. Rev. Plant Biol. **61:** 209–234.

Zeeman, S.C., Northrop, F., Smith, A.M., and Rees, T. (1998a). A starch-accumulating mutant of *Arabidopsis thaliana* deficient in a chloroplastic starch-hydrolysing enzyme. Plant J. **15:** 357–365.

Zeeman, S.C., Umemoto, T., Lue, W.L., Au-Yeung, P., Martin, C., Smith, A.M., and Chen, J. (1998b). A mutant of *Arabidopsis* lacking a chloroplastic isoamylase accumulates both starch and phytoglycogen. Plant Cell **10:** 1699–1712.

Zhao, J., Liu, Q., Zhang, H., Jia, Q., Hong, Y., and Liu, Y. (2013). The rubisco small subunit is involved in tobamovirus movement and Tm-2^2-mediated extreme resistance. Plant Physiol. **161:** 374–383.

Ziegler, P., and Beck, E. (1986). Exoamylase activity in vacuoles isolated from pea and wheat leaf protoplasts. Plant Physiol. **82:** 1119–1121.